UC Merced

UC Merced Previously Published Works

Title

Differential capacity of kaolinite and birnessite to protect surface associated proteins against thermal degradation

Permalink

https://escholarship.org/uc/item/75k1f2j1

Authors

Chacon, Stephany S
García-Jaramillo, Manuel
Liu, Suet Yi
et al.

Publication Date

2018-04-01

DOI

10.1016/j.soilbio.2018.01.020

Peer reviewed

eScholarship.org Powered by the California Digital Library
University of California

THE FATE OF PROTEIN AT MINERAL SURFACES: INFLUENCE OF PROTEIN CHARACTERISTICS, MINERALOGY, PH, AND ENERGY INPUT

Stephany Soledad Chacon[a*]

Manuel Garcia Jaramillo Rodriguez[a]

Suet Yi Liu[b]

Musahid Ahmed[b]

Markus Kleber[ac]

[a] Department of Crop and Soil Science, Oregon State University, Corvallis OR 97331 United States

[b] Chemical Science Division, Lawrence Berkeley National Laboratory, Berkeley, CA, 94720 United States

[c] Institut für Bodenlandschaftsforschung, Leibniz Zentrum für Agrarlandschaftsforschung (ZALF), Eberswalder Straße 84, 15374 Müncheberg, Germany

*Corresponding Author

Email: Stephany.chacon@oregonstate.edu

Abstract

Soil organic carbon cycling depends on the presence and catalytic functionality of extracellular proteins. The mineral matrix has the capacity to enhance, maintain or impede this functionality through a variety of mechanisms. The goal of this research was to identify some of the mechanisms involved in determining the role of the mineral matrix towards proteins. To this end, we adsorbed Beta-Glucosidase (BG) and Bovine Serum Albumin (BSA) on the phyllosilicate kaolinite and the manganese oxide acid birnessite at pH 5 and pH 7. The protein-mineral samples were then subjected to gradual energy inputs equivalent to an intense forest fire using a laser and the abundance and molecular masses of desorbed organic compounds were recorded after ionization with tunable synchrotron ~~ultravacuum~~ vacuum ultraviolet radiation (VUV). We found that the mechanisms controlling the fate of proteins varied with mineralogy. Kaolinite adsorbed protein largely through hydrophobic interactions and produced negligible amounts of desorption fragments compared to birnessite, even at energy inputs equivalent to an intense forest fire. Acid birnessite adsorbed protein through coulombic forces at low energy levels, became a hydrolyzing catalyst at low energies and low pH and eventually turned into a reactant involving disintegration of both mineral and protein at higher energy inputs. Fragmentation of proteins was energy dependent, and did not occur below an energy threshold of 0.20 MW cm^{-2}. Neither signal abundance nor signal intensity were a function of protein size. Above the energy threshold value, BG adsorbed to birnessite at pH 7 showed an increase in signal abundance with increasing energy applications.. Signal intensities differed with adsorption pH for BSA but only at the highest energy level applied. Our results indicate that proteins adsorbed to kaolinite are likely to remain intact

after exposure to the energy loads that may be experienced in natural wildfires. Protein fragmentation and concomitant loss of functionality must be expected in surface soils replete with pedogenic manganese oxides. It is conceivable that a 'fire-activated' mineral matrix may substitute some of the oxidative functionality towards organic matter that may have been lost in the course of protein fragmentation.

1. Introduction

The paradigm of “mineral control” (Torn et al. 1997) posits that the mineral matrix protects soil organic matter (SOM) against microbial decomposition by regulating accessibility and bioavailability of organic substrates through the processes of aggregation and adsorption. Past research into the phenomenon has concentrated on the stabilizing effects of the mineral matrix (Baldock and Skjemstad, 2000; Basile-Doelsch et al., 2007; Doetterl et al., 2015; Dungait et al., 2012; Kemmitt et al., 2008; Marin-Spiotta et al., 2008; Rasmussen et al., 2006; Schmidt et al., 2011; Torn et al., 2013), i.e. the ability of minerals to retard the decomposition of organic substrates. But this research focus is contrasted by long standing evidence for the ability of certain soil minerals to do the exact opposite: promote organic matter degradation by effectively oxidizing (Stone, 1987) and hydrolyzing (Torrents and Stone, 1993) a plethora of organic compounds. Apparently, the mineral matrix has a fundamental capacity to do both: protect organic substrates from decomposition as well as facilitate their disintegration.

Here we attempt to reconcile this apparent contradiction for a group of biomolecules that soil microorganisms deliberately release into the soil pore space to perform functions of critical importance to the ecosystem: extracellular enzymes. Extracellular enzymes are proteins designed to depolymerize soil organic matter (SOM) down to a molecular size small enough to enable passage ~~of~~ through the cell wall for full mineralization. To successfully complete their task, extracellular enzymes need to be able to remain active within the soil pore space over reasonable time scales. This in turn means they must be able to survive contact with mineral surfaces with little or minor impediments to their biological functionality. In fact, eventual sorptive attachment to

mineral surfaces is not necessarily a bad outcome. Often a decrease in the catalytic activity of enzymes is observed upon adsorption (Quiquampoix, 2008), but this tends to go in hand with some degree of protection of the enzyme against microbial predation. Hence an extension of functional life span may result, usually at a somewhat lesser degree of catalytic efficiency than for the free enzyme (Yan et al., 2010), with some noteworthy exceptions where enzymes have greater reaction rates when adsorbed then when free (Allison, 2006; Fiorito et al., 2008). In short, attachment to mineral surfaces appears to be both inevitable and a necessary part of the functional strategy for many, if not all extracellular enzymes. But what if an enzyme encounters one of those minerals that have the demonstrated ability (Sunda and Kieber 1994, Miltner et al 1999) to either oxidize or hydrolyze organic substrates?

Phyllosilicates may be seen as agents of protection due to their sorptive capacity but some have been observed to catalyze the oxidation of aromatic amines, degrade pesticides and dehydrate glucose (Filip et al., 1977; Gonzalez and Laird, 2006). Oxidation sites for phenolic compounds are thought to be located on the crystal edges of phyllosilicates, where transition metals within the octahedral layers are exposed. Phyllosilicates may also concentrate oxygen molecules or reactive oxygen species on their surfaces, which can facilitate the oxidation of aromatics compounds (Thompson and Moll, 1973). In temporarily reducing environments, Fe-oxides may become sources of Fe (II), which can become involved in the oxidation of SOM through Fenton reactions and can increase short-term C mineralization up to 270%. (Hall and Silver, 2013). While phyllosilicates and pedogenic Fe-oxides are conventionally seen as protective of organic matter with some minor potential for indirect enhancement of degradation, the opposite

97 can be said for manganese oxides. The most common clay-sized Mn (IV) oxide in soil,
98 birnessite, has been observed to cleave aromatic rings in phenols, polycyclic aromatic
99 hydrocarbons and other aromatic derivatives through oxidation reactions (Chang Chien et
100 al., 2009; McBride, 1989; Rao et al., 2008; Stone, 1987; Villalobos et al., 2014). The
101 dissolved organic carbon (DOC) from forest litter lost aromatic functional groups after
102 interacting with birnessite (Chorover and Amistadi, 2001). Alkali extracted and
103 operationally defined "fulvic" and "humic" substances interacted with manganese oxide
104 to yield acetaldehyde, pyruvate, and formaldehyde (Sunda and Kieber, 1994).

105 Reports of the fate of proteins at oxidizing/hydrolyzing mineral surfaces are
106 scarce but particularly revealing. A prion protein was fully fragmented in soil upon
107 interacting with birnessite in solution at pH 5 (Russo et al., 2009). Protein disintegration
108 after contact with birnessite surfaces was recently corroborated by Reardon et al. (2016)
109 and the mechanism of fragmentation identified as hydrolysis. The reports of Russo et al
110 (2009) and Reardon et al. (2016) are in contrast to the work of Naidja et al. (2002), who
111 identified birnessite as a strong adsorbent for protein. If we assume both types of
112 observations to be valid, i.e. when birnessite can act towards protein as both, protective
113 sorbent and fragmenting catalyst, then we need to identify mechanisms and
114 circumstances that determine when a mineral surface changes its role.

115 To constrain this issue it is useful to recall that the main mechanisms of protein –
116 mineral interactions include hydrogen bonding, electrostatic attraction and repulsion,
117 hydrophobic interactions, and entropy driven conformational change (Chaperon et al
118 2013, Boyd and Mortland 1990, Craig and Collins 2002). Among these four mechanisms,
119 electrostatic interactions are the ones that are most susceptible to environmental controls

such as soil pH and should therefore receive particular attention. The remaining three factors (hydrophobic interactions, hydrogen bonding and ability to change conformation upon adsorption) are largely determined by protein type and molecular size (Balcke et al., 2002; Sander et al., 2010). We deduced that an attempt to investigate the requirements for an abrupt change in the quality of mineral – organic interactions should include some variation in protein size and in protein responsiveness to electrostatic forces, the former reflected in molecular mass and the latter modified by variation of the isoelectric point of the protein (Norde, 2008; Quiquampoix et al., 1995). We further decided to vary energy input to the system based on a recent observation of temperature-induced variation in the abiotic reactivity of mineral surfaces. This phenomenon was observed by Bach et al. (2013) and Blankinship et al (2014) who independently performed measurements of polyphenol oxidase (PPO) and peroxidase (PER) enzyme acitivities in soil samples. In their attempt to quantify any background contribution of the mineral matrix, Bach et al. (2013) and Blankinship et al. (2014) autoclaved and/or combusted their soils to sterilize and completely denature the enzymes and thus eliminated any enzymatic contribution to their assays. Yet some of the combusted and autoclaved soils degraded the aromatic test substrate (L-DOPA) to a larger extent than the living, enzyme bearing soils, with soils combusted at 500 °C showing greater efficacy than autoclaved soils. This observations led us to speculate that external energy input, as it occurs in the topsoils of many fire–prone ecosystems, may have the potential to enhance the general capacity of the mineral matrix to fragment organic matter and may potentially act to convert “sorptive” into “reactive” mineral surfaces.

Consequently, the overarching goal of this research was to contribute to a mechanistic understanding of the dual role of mineral surfaces as both (i) stabilizing agents for soil protein and (ii) catalysts or reactants involved in their abiotic fragmentation. Previous evidence from Russo et al (2007) and Reardon et al (2016) indicates that acid birnessite has the capacity to fragment proteins in aqueous systems, but did not investigate the reactivity of minerals towards proteins in the absence of the aqueous phase, such as in periodically dry topsoils. Hence, our conceptual approach was to document the fate of protein on dry mineral surfaces of different potential surface reactivity while varying four known controls on protein-mineral interactions:

(i) protein size (measured in kDa),
(ii) mineral surface type (sorbent type versus known catalyst/reactant type mineral)
(iii) surface charge status of proteins and minerals as controlled by soil pH (varying pH as well as the isoelectric point of the proteins and the point of zero charge of the minerals),
(iv) the energy input to the protein-mineral association (subjecting the protein-mineral system to progressively higher inputs of precisely dosed laser energy)

Our experimental design consisted of reacting two types of protein with two kinds of minerals in a slurry at two pH levels bracketing the main pH region for many soils (pH 5 and pH 7). After drying on an inert silica wafer, the protein-mineral mixtures were inserted into a vacuum chamber, subjected to a defined input of laser energy and the abundance and chemical composition of desorbed organic compounds was recorded after VUV ionization using a time of flight Mass Spectrometer. To do so, we took advantage of a ~~respective~~ experimental setup at Beamline 9.0.2 of the Advanced Light Source at Berkeley, CA. Our experimental approach allowed us to test the following hypotheses:

(1) The extent of protein adsorption at a mineral surface will be proportional to the extent of attractive electrostatic interactions.

(2) With constant protein size and pH, fragmentation is a function of mineralogy, even in the absence of an aqueous phase.

(3) The number of peptide signals in the mass spectrum is a function of

a) protein size (constant energy and pH)

b) pH (constant energy and protein size)

c) energy applied (constant protein size and pH)

(4) With constant protein size and pH, the intensity of signals in the mass spectum is a function of energy applied.

2. Materials and Methods

We selected Beta Glucosidase (BG) and Bovine Serum Albumin (BSA) to achieve variation in size and isoelectric point (pI) of the protein. These were adsorbed to acid birnessite (catalyst/reactant type mineral) and kaolinite (sorbent type mineral). The proteins were allowed to interact with the minerals at pH 5 and pH 7 to create variation in the extent of electrostatic attraction and repulsion between constituents (Figure 1).

Figure 1

Insert here

2.1 Materials

Beta-glucosidase and Bovine Serum Albumin were obtained from Sigma Aldrich and used directly from their containers. Acid Birnessite was synthesized using the protocol described by Villalobos et al. (2003) and purified with a 1000 kDa dialysis tube until conductivity of supernatant was less than 40 μS cm^{-1}. The dialyzed acid birnessite was freeze-dried and stored at room temperature in amber glass bottles. Kaolinite (KGa-1b) was ordered from the Clay Minerals Society Source Clays and exchanged with sodium chloride. The Na-kaolinite was washed until ionic conductivity was less than 40 μS cm^{-1} and freeze-dried. The point of zero charge for acid birnessite was measured using Prolonged Salt Titration (PST) method (reported in SI). The general properties of the protein and minerals are reported in Table 1.

[Insert Table 1 here]

2.2. Development of a variable to quantify the extent of electrostatic attraction

To assess the dependence of protein adsorption on electrostatic attraction, we developed a simple procedure to estimate the extent of opposite charge overlap between the protein and the mineral. The underlying reasoning is as follows. Maximum electrostatic attraction between a protein and a mineral will occur when the total net surface charge of either reaction partner has opposite sign, a situation that we consider as "maximum overlap of opposing charges". At pH ranges typically found in soils, the proteins and minerals chosen for this study will carry variable proportions of both, positive and negative charges. In our system, a situation of near total overlap (i.e. one reactant being overwhelmingly positively charged while the other is overwhelmingly

negatively charged) occurs at pH 5, where both minerals are negatively charged and beta-glucosidase is positively charged (Figure 1). The degree of 'charge overlap' given in Figure 1 was calculated as follows: The *fraction of positive charge on the protein* (Y_B) was calculated with equation 1 using the protein's isoelectric point (pI).

$$Y_B = Total\,Charge \times \frac{1}{\left(1+10^{(pH-pI)}\right)} \quad (1)$$

The *fraction of positive charge on the mineral* (Y_A) was calculated with equation 2 using the mineral's point of zero charge (PZC). The *fraction of negative charge on the mineral* (X_A) was then calculated by subtracting the positive charge from the total charge, which was set at unity (Equation 3). The positive charge of the protein was subtracted from the total charge (also at unity) to yield the *fraction of negative charge of the protein* (X_B). The fractions of charge are indicated in Table 2.

$$Y_A = Total\,Charge \times \frac{1}{\left(1+10^{(pH-pzc)}\right)} \quad (2)$$

$$X_B = Total\,Charge - Y_B \quad (3)$$

$$X_A = Total\,Charge - Y_A \quad (4)$$

These values were used to calculate the extent of opposite charge overlap between protein and minerals (α) at typical soil pH values of 5 and 7, using Equation 5. The overlap of opposite charges can be seen as a coarse proxy for the potential strength of electrostatic attractions between the proteins and the minerals.

$$\alpha = \left|X_B - X_A\right| \approx \left|Y_B - Y_A\right| \quad (5)$$

The α values generated in equations 5 are reported for our experimental set up as proportion of total charge and reported as a percentage (Figure 1).

2.3 Development of a variable to estimate potential contribution of conformational change to protein adsorption

Soft proteins undergo conformational change upon adsorption onto a surface. occur at a pH near or at the isoelectric point of a protein. At the isoelectric point, volume can shrink in size, which allows more molecules to be packed onto a surface (Norde 2008). We defined the difference between the adsorption pH and the pI as a proxy for eventual conformational change (ν). As pH nears the pI or ν is smaller, we expect volume changes (ν) to have greater influence on the amount of protein adsorbed (q)

$$\upsilon = f\left|pH_{Adsorption} - pH_{pI}\right| \quad (6)$$

2.4 Protein adsorption to mineral surfaces

Protein-mineral samples were prepared at pH 5 with 100 mM sodium acetate and pH 7 with 100 mM TRIS buffer. Beta-Glucosidase (BG) and Bovine Serum Albumin (BSA) were dissolved in buffers at a concentration of 3 mg/mL (C_i). The 1.00 mL of protein solution was mixed for every 20 mg of Kaolinite and Acid Birnessite ($m_{mineral}$). The samples were mixed and allowed to sit for 24 hours at 20 °C. Unadsorbed protein was removed by centrifuging at 11,700 rcf for 40 minutes and pipetting out the supernatant. The concentration of protein in the supernatant, or the equilibrium (C_{eq}) was determined using UV-Vis spectroscopy at 280nm. The protein-mineral pellets were

washed with buffer by re-suspending the pellet and centrifuging the samples. The supernatant was removed and the process was repeated once more. The amount of protein adsorbed onto the mineral surfaces were calculated with the following equation:

$$q = \frac{volume\left(C_i - C_{eq}\right)}{m_{mineral}} \quad (7)$$

To test the effects of electrostatic interactions on protein adsorption, we performed linear regression analyses to obtain slopes, coefficients of determination, and P-values for the dependence of q on electrostatic interaction parameters. Multi linear regressions analysis was also used to test whether there were significant interactions between parameters.

2.5 Laser Desorption Post Ionization Mass Spectrometry of Protein-Mineral samples

Sample preparation for laser desorption post-ionization mass spectrometry (LDPI-MS) was done by suspending the protein-mineral pellets with 1.0 mL MilliQ water. The suspension was transferred to a silicon wafer and allowed to dry in a desiccator for 2 days before analysis by LDPI-MS. The samples were placed on the platform in the LDPI-MS and analyzed under vacuum. A 349 nm Nd:YLF laser with a focus spot of ~15 μm was used to irradiate the sample at 8.5 ns pulses using linear raster scanning over 18 mm at a rate of 2mm/s with the laser at varying energy levels. Expressed in commonly used power density units, the energy applied spanned a range from 0.05 to 1.84 MW cm^{-2}. To relate experimental settings to the conditions observed during natural wild fires, power densities were converted to fire line intensity units (kW m^{-1}) defined as the rate of energy or heat release per unit length of fire front (Byram, 1959). A conversion table is provided in Table S4.

The fragments desorbed by the laser were then ionized with vacuum ultraviolet radiation (VUV) at a constant energy of 10.5 eV (Liu et al., 2013). The ions were then detected with the mass spectrometer with a detection limit of 3000 mass per charge (m/z).

We used the following parameters to interpret and describe the results from LDPI-MS analysis. The ***total ion count*** *(TIC)* is the number of peaks times their intensity (unit: total detector counts) and is used to describe the magnitude of overall signal generation. The ***signal intensity*** parameter is the magnitude of a single peak (unit: counts per specific mass), which provides the contribution of single mass to the mass spectrum. Finally, we use the term ***signal abundance*** (unit: number of signals of interest observed) to refer to the number of individual discernable peaks as a proxy for the extent of fragmentation.

3. Results

3.1 Charge overlap and conformational change explain protein adsorption

The amount of protein adsorbed on kaolinite decreased in a strong linear relationship as α increased (Figure 2A). This was contrasted with the strong positive linear relationship observed between α and protein adsorption onto birnessite. The relationship between q and α was statistically significant for both minerals at $p < 0.01$. The influence of conformational change (ν) to protein adsorption is illustrated by plotting q as a function of ν (Figure 2B). There was a slight increase in q for kaolinite samples when pH was closer to the pI (Figure 2C). A similar weak linear relationship between q and ν was observed for birnessite samples (Figure 2D). When fitting a linear function, a trend was apparent which was not statistically significant. A multilinear regression model

including interactions between opposite charge overlap (α) and conformational change (ν) were able to explain 90 % of variability for kaolinite samples. The same multi linear regression model for birnessite explained 68% of the variability in the data (Table S1).

[Insert Figure 2 here]

3.2 Total ion counts and mass spectra include signals from buffer and birnessite

Laser application to birnessite control samples (birnessite plus sodium acetate and birnessite plus Tris buffer) released ions with masses greater than 200 Dalton (Figure 3) in the absence of protein. Such behavior was not observed on kaolinite samples. Birnessite plus Tris buffer had signals at 355.07, 428.98, 502.95, 552.95 and 626.90 m/z (Figure 3J-3I). The signals at 552.95 and 626.90 m/z were similarly found on birnessite samples with sodium acetate buffer along with new signals at 405.01 and 479.14 m/z (Figure 3K-3L). As these signals reached intensities comparable to signal intensities from protein-birnessite samples, the mass spectra of protein-mineral samples had to be scrutinized for *unique signals* that were not present in the mineral-buffer samples and only found in protein-containing samples (Figure 3).

[Insert Figure 3 here]

3.3 The abundance of fragmentation products is a function of energy applied

It was possible to release compounds into the gas phase and subsequently ionize them using VUV radiation at all levels of energy input (0.05-1.84 MW cm^{-2}). Total ion counts

from mineral and protein phases generally increased with higher energy application, with some exceptions (Table 3). Unique signals from protein containing birnessite samples were not detected at energies below 0.20 MW cm^{-2} (Figure S4). Application of 1.28 MW cm^{-2} to BG samples at pH 7 did not generate unique signals from protein samples. When the laser energy was increased from 1.28 MW cm^{-2} to 1.84 MW cm^{-2}, unique signals at 408.31 m/z and 707.22 m/z appeared from BG at pH 7 (Figure 3F). For BG-birnessite samples at pH 5, increasing the energy level did increase the signal abundance of unique masses arising from protein containing samples (Figure 3G-H). The mass spectrum generated after applying 1.28 MW cm^{-2} to BSA adsorbed onto birnessite at pH 7 contained unique signals between 233.09 to 700.9 m/z (Figure 3A). When the energy was increased to 1.84 MW cm^{-2}, new signals between 602.21 to 786.33 m/z appeared in BSA-birnessite samples adsorbed at pH 7 (Figure 3B). The BSA-birnessite-pH5 combination returned unique signals at 222.13 m/z, 244.26 m/z, and 429.47 m/z when 1.28 MW cm^{-2} of energy was applied (Figure 3C). Higher energy applications increased the unique signal abundance of the BSA-birnessite-pH 5 combination (Figure 3D). In general, increasing the energy application to BG- and BSA-birnessite samples adsorbed at pH 5 increased the signal abundance detected and the signal intensity of some peaks.

[Insert Table 3 here]

3.4 Protein fragmentation patterns differ between mineral surfaces

The majority of ionized compounds from protein-mineral samples were detected within a range of 0 to 1500 mass per charge (m/z). Signal intensities returned from

protein-birnessite combinations were significantly higher than those obtained from proteins adsorbed to kaolinite or Si wafer surfaces, which did not generate signal intensities above the noise level unless subjected to an energy density of 1.84 MW cm^{-2}). For this reason, all comparisons between protein-mineral combinations (Figure S5) were performed at that energy level. The maximum count intensities in the mass spectra generated for Si wafer and kaolinite samples were lower than 100 counts. But, depending on adsorption pH and type of protein, birnessite-protein samples samples returned total ion counts between 800 to 3600.

[Insert Figure 4 here]

3.5 *Fragmentation signal intensities are not necessarily a function of protein size*

Neither signal abundance nor total ion counts were a function of protein size Mass spectra obtained from protein –birnessite combinations at power denisties above 0.20 MW cm^{-2} were the only ones that had unique signals above the noise level. Among samples that had been adsorbed at pH 5, BG (135 kDa)-birnessite specimens generated higher total ion counts (TIC) than BSA (66.5 kDa)-birnessite samples (Table 3). At an adsorption pH of 7, BG-Birnessite TIC were higher than BSA-Birnessite at energy levels below 0.68 MW cm^{-2} (Table 3). Above this energy, the smaller protein (BSA) generated greater total ion counts than the larger protein (BG). The BSA-birnessite samples showed greater unique signal abundance than BG-birnessite samples at pH 7 (Figure 3). Only at the highest energy application did BG-birnessite samples at pH 5 surpass the unique signal abundance of BSA-Birnessite samples at pH 5.

[Insert Figure 4 here]

3.6 pH dependence of protein fragmentation

The only samples that had greater signal abundance at an acidic adsorption pH were BG-birnessite samples; for BSA-birnessite the signal abundance at pH 7 was greater than that at pH 5. BG adsorbed at pH 5 yielded greater TIC than BG adsorbed at pH 7, as energy was held constant (Table 3). We also noticed the presence of unique signals in the BG-birnessite mass spectrum at pH 5 that were not present for samples at pH 7 (Figure 3E-3H). In BSA-Birnessite samples, TIC was higher for samples at pH 5 than pH 7 when the energy levels were below 0.20 MW cm^{-2}, but these total ion counts were primarily made up of signals from the buffer and birnessite. The TIC from BSA-birnessite samples at pH 7 surpassed TIC from samples at pH 5 when energy levels reached 0.20 MW cm^{-2}. At 1.28 and 1.84 MW cm^{-2}, BSA-birnessite specimens produced higher unique signal intensities at pH 7 than pH 5 (Figure 3A-3D).

3.7 Total ion counts as a function of power density

On all three mineral surface types, adsorbed protein generated largely similar total ion counts (TIC) as long as power densities were below 0.20 MW cm^{-2}. Protein-birnessite combinations showed an exponential increase in total ion counts when power density was increased beyond ~~beyond~~ 0.20 MW cm^{-2}. But once energy applications were above that threshold, TIC from birnessite was generally higher than from kaolinite samples or Si wafer samples within the same energy level (Figure 5). In samples containing only

birnessite with buffer added, we observed an exponential increase of TIC with increasing energy (Figure 5). The TIC from kaolinite controls (mineral plus buffer) were much lower than the TIC from birnessite controls. For protein-birnessite at pH 5, higher TIC was detected than from birnessite controls. At pH 7, TIC from the birnessite control was mostly higher than TIC from protein-birnessite TIC with the exception of the birnessite-BSA combination at pH 7. Once an energy threshold of 0.20 MW cm^{-2} was reached, TIC from BSA birnessite samples at pH 7 was higher than the TIC from the birnessite control and the TIC from the BG-Birnessite combination at pH 7. Addition of protein to kaolinite samples and subsequent exposure to a gradient of laser energies actually decreased the TIC in comparison to the TIC from the kaolinite control. This occurred regardless of pH or energy applied. The TIC detected from proteins added to polished Si wafers increased with application of laser energy. The TIC for protein-Si wafer combinations was similar between proteins and pH with the exception of BSA at pH 5. There was a decrease in TIC when laser energy went below 0.20 MW cm^{-2} for the BSA-Si wafer combination for pH 5 samples. TIC from Si wafer combinations were similar in magnitude to TIC from Kaolinite samples. Overall, protein-birnessite combinations had much higher TIC than protein-kaolinite or protein-Si wafer combinations when applying energy above the 0.20 MW cm^{-2} threshold.

[Insert Figure 5 here]

4. Discussion

4.1 Adsorption mechanisms and protein fragmentation are mineral dependent

The extent of charge overlap predicted protein adsorption in kaolinite and in birnessite. In kaolinite samples, more protein was adsorbed when protein and mineral had like charges, in birnessite, the opposite was observed (Figure 2 a,b). This apparent contradiction can be rationalized by considering significant differences in surface charge characteristics and the surface area between these minerals (Table 1). Acid birnessites have a larger reservoir of negative charge on its surface, between 63 to 240 meq_{charge} $100g^{-1}$[1], compared to kaolinite's reservoir of 3.0 meq_{charge} $100g^{-1}$ (Borden and Giese, 2001; Golden, 1986). Kaolinite contains very little permanent negative charge on its basal siloxane surface. The siloxane surface of kaolinite has greater hydrophobic character than other phyllosilicates with greater permanent charge from isomorphic substitution. (Jaynes and Boyd, 1991). This hydrophobic character was found to be responsible for the irreversible adsorption of operationally defined "humic substances" onto kaolinite (Balcke et al 2002). Thus, conditions disfavoring electrostatic attraction could favor hydrophobic interactions between proteins and kaolinite. The contrasting results between α and q indicate that the controlling mechanisms for protein adsorption differ between kaolinite and birnessite.

The appearance of unique signals from protein-mineral combinations is interpreted as evidence of protein fragmentation. We **found** that unique signals were only in acid birnessite samples and not kaolinite, making protein fragmentation mineral dependent as well. Past research has identified birnessite as a sorbent for protein (Naidja et al., 2002), but more recent evidence has shown birnessite can break apart proteins in acidic aqueous systems (Russo et al 2009) and generate peptide fragments < 1000 Da (Reardon et al 2016). Kaolinite seems to function as a sorbent even after energy

applications that simulate intense forest fires. Our research also exhibits the dichotomy of birnessite by confirming the importance of both pH (greater mineral reactivity with lower pH) and energy input (change from passive sorbent to chemical reactant) for the overall reactivity of birnessite.

4.2 Birnessite is more susceptible to disintegration than kaolinite

Contrary to kaolinite controls (= kaolinite plus buffer), birnessite controls (birnessite plus buffer) responded to energy input with the production of signals that were tentatively identified as organomanganese complexes (see Supplemental Information). The breakdown of birnessite as the energy application increases makes it less likely to be a candidate for a catalyst. The susceptibility of birnessite to disintegrate after applying increasing amounts of energy was muted in the presence of protein. This phenomenon can be rationalized by considering the significantly lower threshold of birnessite for mineral transformations. Temperatures must reach 550°C until dehydroxylation occurs in kaolinite and 1000°C until it transforms into the aluminum oxide Mullite (Insley and Ewell 1935, Glass 1954). In contrast, the dehydration of the birnessite surface and interlayers occurs between the temperatures of 25°C-200°C, which can modify the layered structure (Ghodbane et al., 2010). We deduce that high laser energies change the role of the mineral birnessite towards proteins from that of a sorbent surface with some catalytic capabilities in aqueous low temperature systems (Reardon et al 2016, Russo et al 2009) to that of a chemical reactant. The energetic threshold for this conversion seems to be in the vicinity of 0.2 MW cm^{-2}.

4.3 Energy dependence of fragmentation shows a threshold

The energy range of 0.20-1.84 MW cm^{-2} used in our experiments equates fireline intensities between 47.8-433.7 kW m^{-1} (Table S3), well within the range of fire line intensities calculated for fires with fuel beds of scrubland, grasslands, and pine litter with grass understory (Alexander and Cruz, 2012). Both signal abundance and total ion counts of all protein-mineral combinations dependent on the applied power density. In previous work, the LDPI-MS technique was able to detect nearly intact DNA and RNA with minimal fragmentation, despite the fact that those molecules were subjected to internal temperatures of above 670 K (Kostko et al 2011). This can be taken to indicate that little fragmentation should be expected even at high energy applications unless the mineral support surface acts as either catalyst or reactant towards the sorbate. We observed an energy threshold at 0.20 MW cm^{-2} where TIC increased exponentially for birnessite samples and the concomitant appearance of unique protein fragmentation products. These products were not observed in kaolinite samples. This could mean that we may not have applied enough energy to observe the threshold phenomena in the kaolinite samples.

Energy input apparently also controls the reaction mechanism between protein and birnessite: At low energy/temperature and circumneutral pH, birnessite may just act as a sorbent. With decreasing pH, but still at low (environmental) energy/temperature, birnessite becomes a catalyst for the hydrolysis of protein. With high energy inputs above a threshold value corresponding to 0.2 MW cm^{-2}, the birnessite crystal structure begins to break apart and the mineral changes its role again to become a reactant forming Mn-organic compounds Protein interactions with kaolinite show minor energy dependence but significant variation between individual proteins and as a function of pH.

4.4 Fragmentation of sorbed protein by acid birnessite is not mediated by hydrolysis

The unique signals found in the mass spectra of protein-birnessite samples did not match hydrolysis reaction products of BSA and BG. Previous studies have demonstrated birnessite's capacity to oxidize biomolecules (Laha and Luthy, 1990) and catalytically cleave proteins through hydrolysis (Reardon et al 2016). We were interested in determining if hydrolysis was still the mechanism responsible for fragmentation of a sorbed protein under dry conditions. If birnessite breaks apart proteins through hydrolysis, the cleavage would be between the amide bonds, generating recognizable peptides and amino acids. But if birnessite oxidizes proteins, the products would not match the hydrolysis byproducts. Protein oxidation could occur through a multitude of pathways that can generate cross-linked proteins, oxidized side chains, carbonylation and fragmentation products that do not align with hydrolysis products (Berlett and Stadtman, 1997). A list of masses generated by hydrolytic cleavage of BSA and BG by Proteinase K, a broad cleavage activity enzyme, was compiled in order to compare them to the unique masses. There were no matches between the unique signals and the hydrolysis products. Even after accounting for possible oxidation of aromatic side chains (Table S5). It is possible that the hydrolyzed peptides, as detected by Reardon et al (2016), could have initially been removed when the supernatant of the unadsorbed protein was separated from the solid phase. We were only observing the fate of residual protein or peptides on the mineral surfaces and not the peptides released into solution. The addition of energy to protein-birnessite samples may shift the mechanism of fragmentation from hydrolysis in low energy and aqueous systems to an oxidative reactant under dry conditions.

4.5 Greater protein size does not lead to more fragmentation products

Laser desorption mass spectrometry has previously been applied to detect fragments from medium range molecules, such as antibiotics, biofilms and peptides (Blaze et al., 2011; Gasper et al., 2010). The LPDI-MS instrument can detect single charge species up to 3000 Dalton. We found protein size did not control the amount of fragmentation products or total ion counts after interaction with a reactive mineral surface. Based on a known positive linear relationship between protein adsorption and the molecular mass of a protein (Harter and Stozky 1971) we initially hypothesized that larger proteins would mean more extensive contact with the mineral surface. The more amino acids in contact with the surface, the greater amounts of fragmentation we expected to observe. Surprisingly, the combination of the smaller protein BSA with birnessite at pH 7 had the lowest amount of protein adsorbed but the highest TIC and unique fragmentation product signals.

4.6 Acidic pH enhances birnessite reactivity for BG

A low adsorption pH enhanced fragmentation and total ion counts for beta-glucosidase (BG) samples but not for Bovine Serum Albumin (BSA). For BG containing samples, fragmentation by birnessite was greater at pH 5 than at pH 7, which is in line with previous observations (Reardon et al. 2016, Russo et al. 2009). Enhanced reactivity of birnessite at acidic pH may be facilitated by increased positive charge of amide functional groups aiding in electrostatic attraction (Laha et al. 1990). But the detection of greater total ion counts and unique signal abundances at 1.84 MW cm^{-2} for BSA samples at pH 7 than pH 5 seems to contradict the previous observations in protein-birnessite

studies. We have no immediate mechanistic explanation for this phenomenon and suggest that it be examined in future investigations.

5. Conclusion

Probably the most significant outcome of our investigation is the insight that protein behavior at mineral surfaces cannot easily be generalized across different minerals. The fate of two proteins differing in mass and surface charge properties was observed to vary individually and as a function of pH, mineral type and energy applied. On kaolinite (a phyllosilicate that can be considered ubiquitous in most soils of the planet), both of the proteins investigated here adsorbed largely through mechanisms other than electrostatic interactions and showed little evidence that their overall response to experimental treatments was significantly modified by the sorbent surface. On birnessite, adsorption occurred mainly through electrostatic interactions. Individual proteins responded differently to the birnessite surface but here their response included fragmentation, whose extent was modified by pH and the magnitude of energy input. Complicating matters further, birnessite appears to change its role in the interaction from sorbent surface over catalyst to chemical reactant, depending on the pH and the energetic status of the system. While our focus was directed at the fate of protein in soil, the observations made also offer some tentative mechanisms for previous observations (Bach et al., 2013; Blankinship et al., 2014), of a significant ability of thermally treated soils to break down other organic substrates.

Acknowledgements

MA, SYL and the Advanced Light Source are supported by the Director, Office of Science, and Office of Basic Energy Sciences, of the U.S. Department of Energy under Contract No. DEAC02-05CH11231. SSC was supported by a Merit Fellowship from the Department of Crop and Soil Science from Oregon State University.

References

Alexander, M.E., Cruz, M.G., 2012. Interdependencies between flame length and fireline intensity in predicting crown fire initiation and crown scorch height. International Journal of Wildland Fire 21, 95-113.

Allison, S.D., 2006. Soil minerals and humic acids alter enzyme stability: implications for ecosystem processes. Biogeochemistry 81, 361-373.

Bach, C.E., Warnock, D.D., Van Horn, D.J., Weintraub, M.N., Sinsabaugh, R.L., Allison, S.D., German, D.P., 2013. Measuring phenol oxidase and peroxidase activities with pyrogallol, L-DOPA, and ABTS: Effect of assay conditions and soil type. Soil biology & biochemistry 67, 183-191.

Balcke, G.U., Kulikova, N.A., Hesse, S., Kopinke, F.D., Perminova, I.V., Frimmel, F.H., 2002. Adsorption of humic substances onto kaolin clay related to their structural features. Soil Science Society of America Journal 66, 1805-1812.

Baldock, J.A., Skjemstad, J.O., 2000. Role of the soil matrix and minerals in protecting natural organic materials against biological attack. Organic Geochemistry 31, 697710.

Basile-Doelsch, I., Amundson, R., Stone, W.E.E., Borschneck, D., Bottero, J.Y., Moustier, S., Masin, F., Colin, F., 2007. Mineral control of carbon pools in a volcanic soil horizon. Geoderma 137, 477-489.

Berlett, B.S., Stadtman, E.R., 1997. Protein oxidation in aging, disease, and oxidative stress. The Journal of biological chemistry 272, 20313-20316.

Blankinship, J.C., Becerra, C.A., Schaeffer, S.M., Schimel, J.P., 2014. Separating cellular metabolism from exoenzyme activity in soil organic matter decomposition. Soil biology & biochemistry 71, 68-75.

Blaze, M.T.M., Takahashi, L.K., Zhou, J., Ahmed, M., Gasper, G.L., Pleticha, F.D., Hanley, L., 2011. Brominated tyrosine and polyelectrolyte multilayer analysis by laser desorption vacuum ultraviolet postionization and secondary ion mass spectrometry. Anal Chem 83, 4962-4969.

Borden, D., Giese, R.F., 2001. Baseline studies of the clay minerals society source clays: cation exchange capacity measurements by the ammonia-electrode method. Clays and Clay Minerals.

Byram, G.M., 1959. Combustion of forest fuels, In: Davis, K.P. (Ed.), Forest fire: control and use. McGraw Hill, New York.

Chang Chien, S.W., Chen, H.L., Wang, M.C., Seshaiah, K., 2009. Oxidative degradation and associated mineralization of catechol, hydroquinone and resorcinol catalyzed by birnessite. Chemosphere 74, 1125-1133.

Chorover, J., Amistadi, M.K., 2001. Reaction of forest floor organic matter at goethite, birnessite and smectite surfaces. Geochimica et Cosmochimica Acta 65, 95-109.

Doetterl, S., Stevens, A., Six, J., Merckx, R., Van Oost, K., Pinto, M.C., Casanova-Katny, A., Munoz, C., Boudin, M., Venegas, E.Z., Boeckx, P., 2015. Soil carbon storage controlled by interactions between geochemistry and climate. Nature Geoscience 8, 780-783.

Dungait, J.A.J., Hopkins, D.W., Gregory, A.S., Whitmore, A.P., 2012. Soil organic matter turnover is governed by accessibility not recalcitrance. Global Change Biology 18, 1781-1796.

Filip, Z., Flaig, W., Rietz, E., 1977. Oxidation of some phenolic substances as influenced by clay minerals. Symposium on Soil Organic Matter Studies.

Fiorito, T.M., Icoz, I., Stotzky, G., 2008. Adsorption and binding of the transgenic plant proteins, human serum albumin, β-glucuronidase, and Cry3Bb1, on montmorillonite and kaolinite: Microbial utilization and enzymatic activity of free and clay-bound proteins. Applied Clay Science 39, 142-150.

Gasper, G.L., Takahashi, L.K., Zhou, J., Ahmed, M., Moore, J.F., Hanley, L., 2010. Laser desorption postionization mass spectrometry of antibiotic-treated bacterial biofilms using tunable vacuum ultraviolet radiation. Analytical chemistry 82, 7472-7478.

Gasteiger, E., Hoogland, C., Gattiker, A., Duvaud, S.e., Wilkins, M.R., Appel, R.D., Bairoch, A., 2005. Protein Identification and Analysis Tools on the ExPASy Server, In: Walker, J.M. (Ed.), The Proteomics Protocols Handbook. Humana Press, Totowa, NJ, pp. 571-607.

Ghodbane, O., Pascal, J.-L.L., Fraisse, B., Favier, F., 2010. Structural in situ study of the thermal behavior of manganese dioxide materials: toward selected electrode materials for supercapacitors. ACS applied materials & interfaces 2, 3493-3505.

Golden, D.C., 1986. Ion Exchange, Thermal Transformations, and Oxidizing Properties of Birnessite. Clays and Clay Minerals 34, 511-520.

Gonzalez, J.M., Laird, D.A., 2006. Smectite-catalyzed dehydration of glucose. Clays and Clay Minerals 54, 38-44.

Grover, A.K., MacMurchie, D.D., Cushley, R.J., 1977. Studies on almond emulsin d-glucosidase I. Isolation and characterization of a bifunctional isozyme. Biochimica et Biophysica Acta (BBA)-Enzymology 482, 98-108.

Hall, S.J., Silver, W.L., 2013. Iron oxidation stimulates organic matter decomposition in humid tropical forest soils. Glob Chang Biol 19, 2804-2813.

Hirayama, K., Akashi, S., Furuya, M., Fukuhara, K.-i., 1990. Rapid confirmation and revision of the primary structure of bovine serum albumin by ESIMS and frit-FAB LC/MS. Biochemical and Biophysical Research Communications 173, 639-646.

Jaynes, W.F., Boyd, S.A., 1991. Hydrophobicity of siloxane surfaces in smectites as revealed by aromatic hydrocarbon adsorption from water. Clays Clay Miner 39, 428-436.

Kemmitt, S.J., Lanyon, C.V., Waite, I.S., Wen, Q., Addiscott, T.M., Bird, N.R.A., O'Donnell, A.G., Brookes, P.C., 2008. Mineralization of native soil organic matter is not regulated by the size, activity or composition of the soil microbial biomass - a new perspective. Soil biology & biochemistry 40, 61-73.

Laha, S., Luthy, R.G., 1990. Oxidation of aniline and other primary aromatic amines by manganese dioxide. Oxidation of aniline and other primary aromatic amines by manganese dioxide.

Liu, S.Y., Kleber, M., Takahashi, L.K., Nico, P., Keiluweit, M., Ahmed, M., 2013. Synchrotron-based mass spectrometry to investigate the molecular properties of mineral-organic associations. Analytical chemistry 85, 6100-6106.

Marin-Spiotta, E., Swanston, C.W., Torn, M.S., Silver, W.L., Burton, S.D., 2008. Chemical and mineral control of soil carbon turnover in abandoned tropical pastures. Geoderma 143, 49-62.

McBride, M.B., 1989. Oxidation of 1, 2-and 1, 4-dihydroxybenzene by birnessite in acidic aqueous suspension. Clays Clay Miner.

Mckenzie, R.M., 1981. The Surface-Charge on Manganese Dioxides. Australian Journal of Soil Research 19, 41-50.

Naidja, A., Liu, C., Huang, P.M., 2002. Formation of protein-birnessite complex: XRD, FTIR, and AFM analysis. J Colloid Interface Sci 251, 46-56.

Norde, W., 2008. My voyage of discovery to proteins in flatland ...and beyond. Colloids Surf B Biointerfaces 61, 1-9.

Putnam, F.W., 1975. The plasma proteins : structure, function, and genetic control, 2d. ed. Academic Press, New York, 141, 147 pp.

Quiquampoix, H., 2008. Interaction with Soil Constituents Determines the Environmental Impact of Proteins. Revista de la ciencia del suelo y nutrición vegetal 8.

Quiquampoix, H., Abadie, J., Baron, M.H., Leprince, F., MatumotoPintro, P.T., Ratcliffe, R.G., Staunton, S., 1995. Mechanisms and consequences of protein adsorption on soil mineral surfaces. Proteins at Interfaces Ii 602, 321-333.

Rao, M.A., Iamarino, G., Scelza, R., Russo, F., Gianfreda, L., 2008. Oxidative transformation of aqueous phenolic mixtures by birnessite-mediated catalysis. Sci Total Environ 407, 438-446.

Rasmussen, C., Southard, R.J., Horwath, W.R., 2006. Mineral control of organic carbon mineralization in a range of temperate conifer forest soils. Global Change Biology 12, 834-847.

Reardon, P.N., Chacon, S.S., Walter, E.D., Bowden, M.E., Washton, N.M., Kleber, M., 2016. Abiotic Protein Fragmentation by Manganese Oxide: Implications for a Mechanism to Supply Soil Biota with Oligopeptides. Environmental science & technology 50, 3486-3493.

Russo, F., Johnson, C.J., Johnson, C.J., McKenzie, D., Aiken, J.M., Pedersen, J.A., 2009. Pathogenic prion protein is degraded by a manganese oxide mineral found in soils. J Gen Virol 90, 275-280.

Sander, M., Madliger, M., Schwarzenbach, R.P., 2010. Adsorption of transgenic insecticidal Cry1Ab protein to SiO2. 1. Forces driving adsorption. Environmental science & technology 44, 8870-8876.

Schmidt, M.W., Torn, M.S., Abiven, S., Dittmar, T., Guggenberger, G., Janssens, I.A., Kleber, M., Kogel-Knabner, I., Lehmann, J., Manning, D.A., Nannipieri, P., Rasse, D.P.,

Weiner, S., Trumbore, S.E., 2011. Persistence of soil organic matter as an ecosystem property. Nature 478, 49-56.

Schroth, B.K., Sposito, G., 1996. Surface charge properties of kaolinite. MRS Proceedings.

Stone, A.T., 1987. Reductive Dissolution of Manganese(III/Iv) Oxides by Substituted Phenols. Environ Sci Technol 21, 979-988.

Sunda, W.G., Kieber, D.J., 1994. Oxidation of Humic Substances by Manganese Oxides Yields Low-Molecular-Weight Organic Substrates. Nature 367, 62-64.

Thompson, T.D., Moll, W.F., 1973. Oxidative Power of Smectites Measured by Hydroquinone. Clays and Clay Minerals 21, 337-350.

Torn, M.S., Kleber, M., Zavaleta, E.S., Zhu, B., Field, C.B., Trumbore, S.E., 2013. A dual isotope approach to isolate soil carbon pools of different turnover times. Biogeosciences 10, 8067-8081.

Torrents, A., Stone, A.T., 1993. Catalysis of Picolinate Ester Hydrolysis at the Oxide Water Interface - Inhibition by Coadsorbed Species. Environmental science & technology 27, 1060-1067.

Villalobos, M., Carrillo-Cardenas, M., Gibson, R., Lopez-Santiago, N.R., Morales, J.A., 2014. The influence of particle size and structure on the sorption and oxidation behaviour of birnessite: II. Adsorption and oxidation of four polycyclic aromatic hydrocarbons. Environmental Chemistry 11, 279-288.

707Villalobos, M., Toner, B., Bargar, J., Sposito, G., 2003. Characterization of the
708manganese oxide produced by< i> pseudomonas putida</i> strain MnB1. Geochimica et
709Cosmochimica ….

710Yan, J., Pan, G., Li, L., Quan, G., Ding, C., Luo, A., 2010. Adsorption, immobilization,
711and activity of beta-glucosidase on different soil colloids. Journal of colloid and interface
712science 348, 565-570.

713Table 1. Properties of the proteins and minerals used in this experiment.

Protein	Isoelectric point (pH)	Molecular Weight (kDa)	Extinction coefficient (M^{-1} cm^{-1})
Beta Glucosidase (BG)	7.3[a]	135[a]	43824[a]
Bovine Serum Albumin (BSA)	5.6[d]	66.4[c]	95310[b]
Mineral	Point of Zero Charge (pH)	Cation Exchange Capacity (meq $100g^{-1}$)	Surface Area (m^2 g^{-1})
Kaolinite (KGa-1)	3.8	3.0[e]	10.05 +/- 0.02[f]
Acid Birnessite	1.92	63-240[g]	40.5 +/- 3[h]

714[a]Grover et al. (1977); [b]Putnam (1975);
715[c]Hirayama et al. (1990); [d]Gasteiger et al. (2005);
716[e]Borden and Giese (2001); [f]Schroth and Sposito (1996);
717[g]Golden (1986); [h]Mckenzie (1981)
718

Table 2. Positive (+) and negative (-) surface charge of protein and mineral surfaces at pH 5 and pH 7 calculated from the point of zero charge (pzc) and the isoelectric point (pI). Values reported as percent total charge and were calculated using equations 1 through 4.

	pH 5		pH 7	
Protein	**+ Charged Surface (%)**	**- Charged Surface (%)**	**+ Charged Surface (%)**	**- Charged Surface (%)**
Beta Glucosidase	99.50	0.5	66.6	33.4
Bovine Serum Albumin	79.92	20.1	3.8	96.2
	pH 5		**pH 7**	
Mineral	**+ Charged Surface (%)**	**- Charged Surface (%)**	**+ Charged Surface (%)**	**- Charged Surface (%)**
Birnessite	0.08	99.9	0.0	100.0
Kaolinite	5.94	94.1	0.1	99.9

Table 3. Comparison between total ion counts of Beta-Glucosidase and Bovine Serum Albumin samples detected off Birnessite at pH 5 and pH 7 with increasing energy applied.

Energy Applied MW cm^{-2}	1/ Energy Applied 1/MW cm^{-2}	Beta-Glucosidase pH 5	Beta-Glucosidase pH 7	Bovine Serum Albumin pH 5	Bovine Serum Albumin pH 7
0.05	19.4	6,355	1,987	4,493	472
0.06	16.2	4,852	2,873	3,532	493
0.07	14.0	5,320	2,318	3,515	538
0.08	12.5	5,083	2,589	3,769	670
0.09	11.1	5,267	2,151	4,295	724
0.16	6.3	5,728	2,862	2,289	884
0.20	4.9	6,507	2,677	2,487	921
0.68	1.5	15,200	7,684	6,580	20,695
1.27	0.8	78,667	80,700	47,871	334,470
1.86	0.5	317,420	315,000	19,916	1,147,200

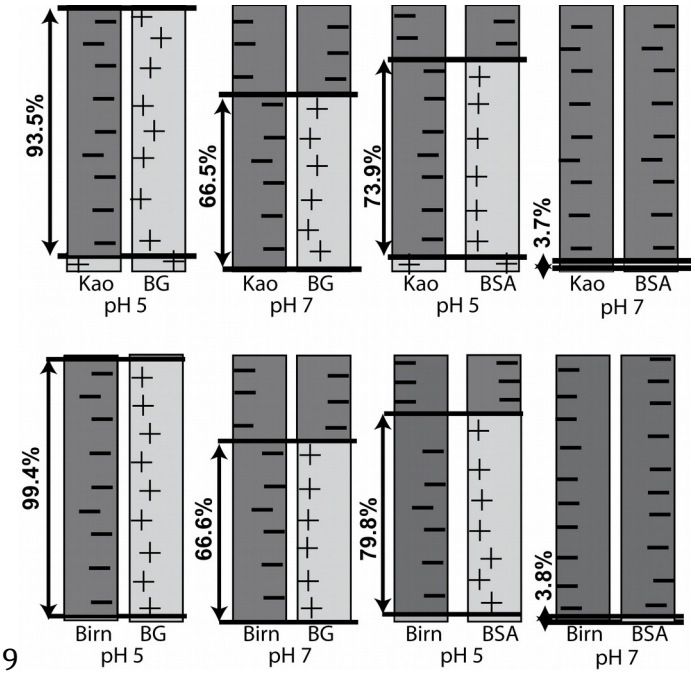

729

730Figure 1 Diagrams indicating potential for attractive electrostatic interactions between
731proteins and minerals at pH 5 and pH 7. Bars with (+) indicate proportion of surface that
732has positive charge. A bar with (-) indicates proportion of surface with has negative
733charge. The proportion of surface charge for Beta-Glucosidase (BG) and Bovine Serum
734Albumin (BSA) were calculated from the isoelectric point and reported in Table 2. The
735proportion of surface charges for Kaolinite (Kao) and Birnessite (Birn) were calculated
736from point of zero charge.

737

738

739

740Figure 2.

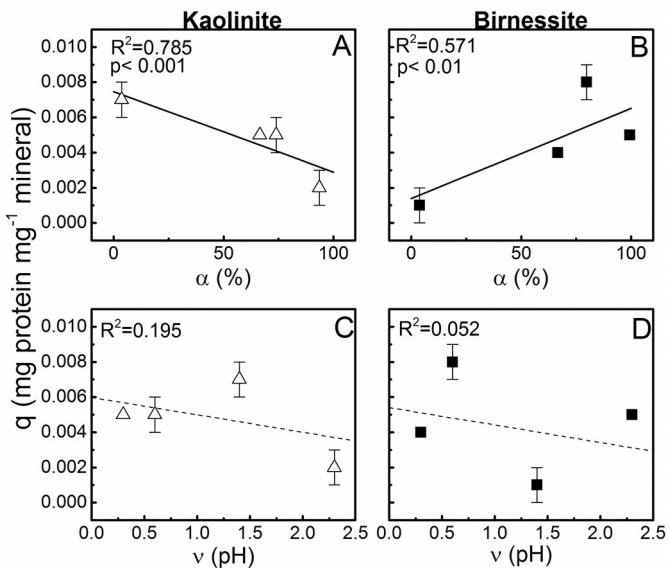

741

742Figure 2. The amount of protein adsorbed onto kaolinite (open triangles) and birnessite
743(closed squares) as a function of opposite overlap charge (α) and the pH distance from the
744isoelectric point (ν). Each symbol represents a mean with an n=3. The error bars represent
745the standard deviation. Bold lines represent strong correlation and dashed lines represent
746weaker correlations.

747

748

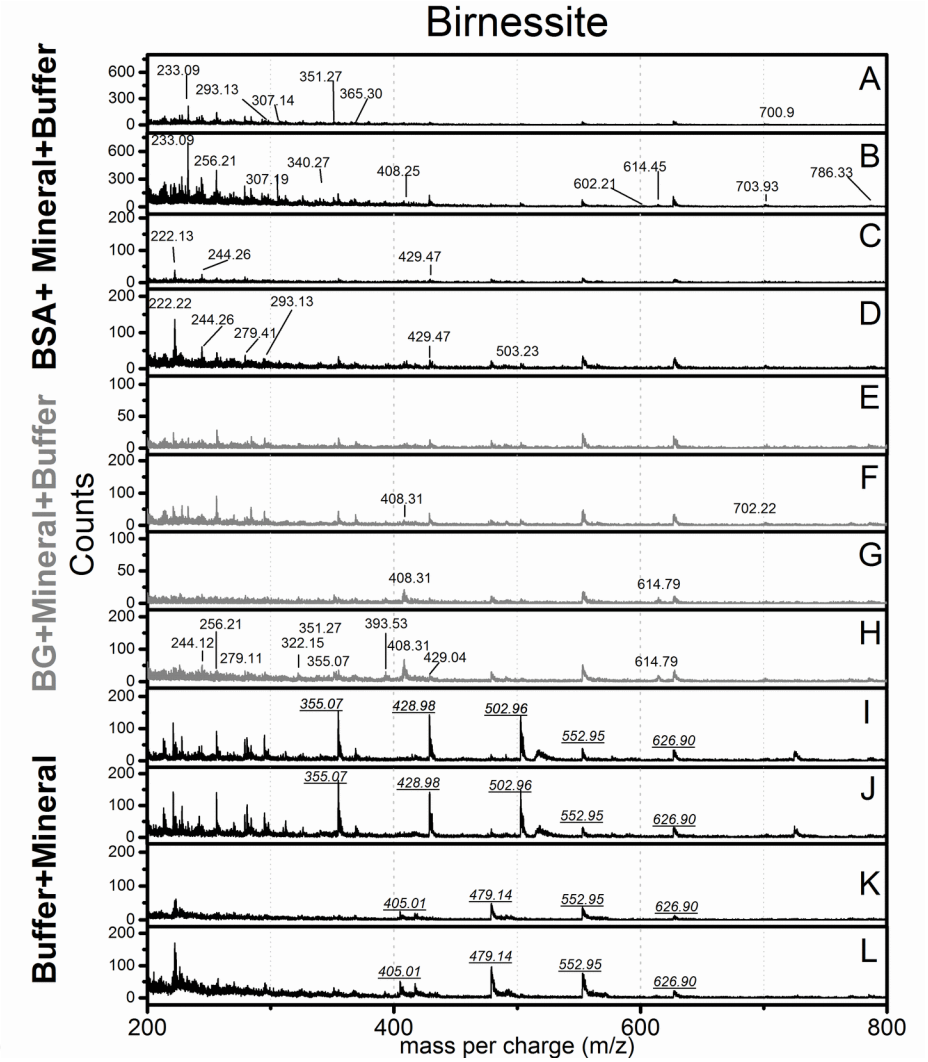

Figure 3. Mass spectra from birnessite+buffer samples (I-L) were compared to protein+birnessite+buffer samples (A-H) to identify the presence of peaks only found in protein containing samples between 200-800 mass per charge (m/z). Samples of Bovine Serum Albumin (BSA) on birnessite containing Tris buffer at pH 7 with A) 1.27 MW cm^{-2} and B) 1.84 MW cm^{-2} energy applied. Similar conditions were used for BSA on birnessite samples with Sodium Acetate buffer at pH 5 for C) 1.27 MW cm^{-2} and D) 1.84 MW cm^{-2}. Mass spectra of Beta-Glucosidase (BG) on birnessite containing Tris buffer with E) 1.27 MW cm^{-2} and F) 1.84 MW cm^{-2} energy applied. Conditions were replicated

759for BG on birnessite containing sodium acetate buffer for G) and H). Samples of
760birnessite containing only Tris buffer at pH 7 released ions when I) 1.27 MW cm^{-2} and J)
76111.84 MW cm^{-2} of energy was applied. Birnessite samples containing sodium acetate at pH
76225 released ions after application of K) 1.27 MW cm^{-2} and L)1.84 MW cm^{-2}. Peaks
763highlighted in birnessite samples containing Bovine Serum Albumin (BSA) and Beta-
764Glucosidase (BG) are unique peaks that are not found in birnessite buffer samples or have
765higher signal intensity than birnessite-buffer peaks. Peaks from birnessite buffer samples
766were underlined. Mass spectra shown here are from the two highest energy applications.

767Figure 4

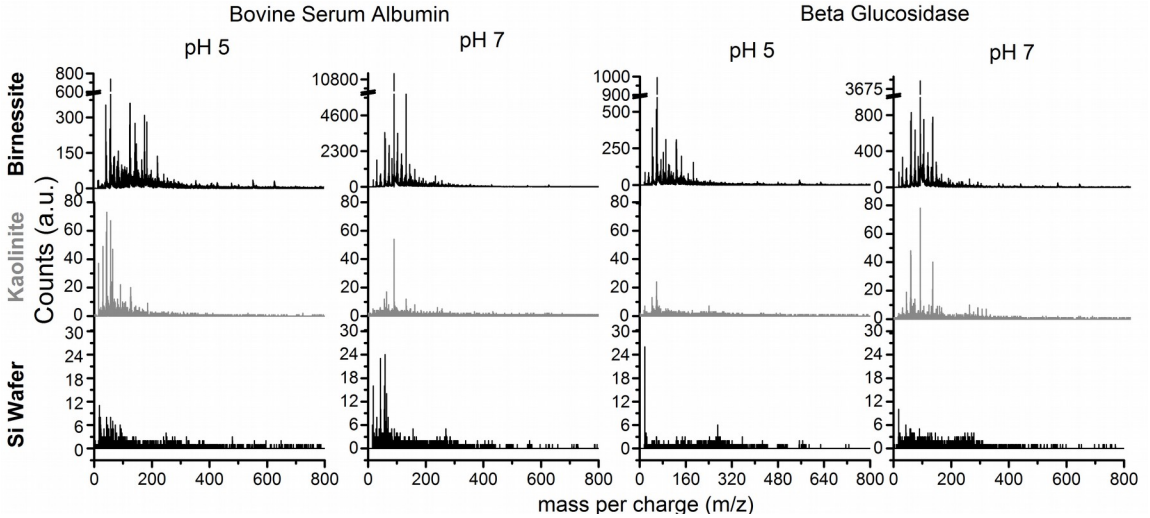

769Figure 4. Comparison between mass spectra from Beta-Glucosidase (BG) and Bovine
770Serum Albumin (BSA) desorbed off Birnessite (top), Kaolinite (middle) and Si wafer
771(bottom) at pH 5 and pH 7. Energy applied to all samples was 1.84 MW cm^{-2}. Breaks
772were at added at 85% of the scale to focus on peaks not from the buffers.

773

774

775

776

777

778Figure 5.

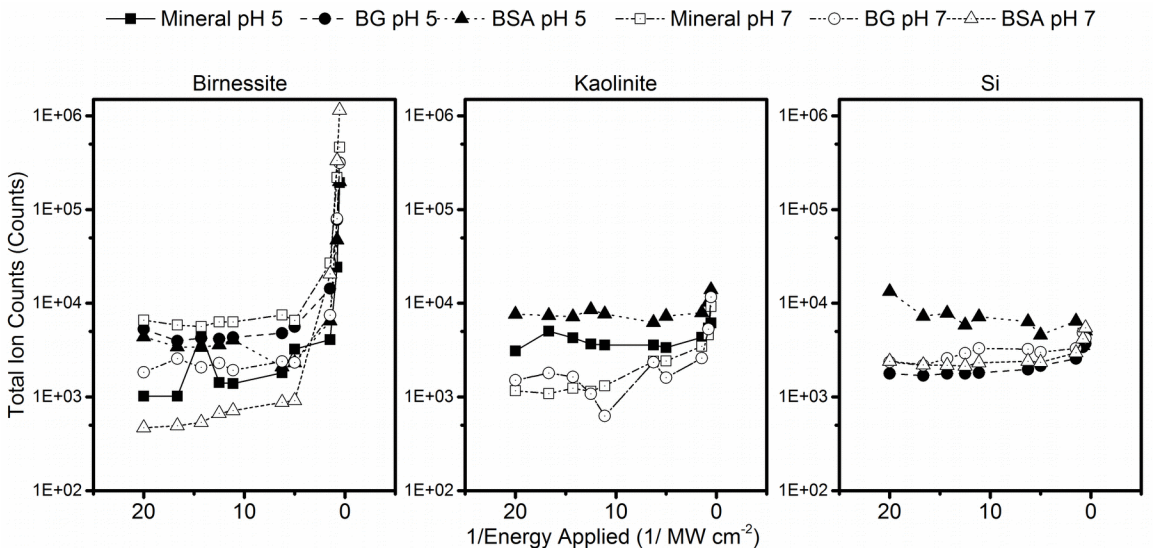

779

780Figure 5 Total Ion counts of samples on birnessite (left), kaolinite (middle), and Si wafer

781(right). X-axis arranged to show increasing application of energy towards the right. TIC

782below energy threshold show linear trend on $\log_{10}$ y-axis. After 0.2 MW cm^{-2}, exponential

783increase of TIC observed.

784